5th Joint International Symposium on Deformation Monitoring (JISDM), 20-22 June 2022, Valencia, Spain
DOI: http://doi.org/10.4995/JISDM2022.2022.13815

Drill bit grading using LiDAR and imagery on the apple smart devices

Fengman Jia[1], Derek D. Lichti[1], Roman Shor[2], Arsh Khawaja[2], Min Kang[1], Max Kepler[3]

[1] Department of Geomatics Engineering, University of Calgary, 2500 University Dr NW, Calgary, AB, T2N 1N4, Canada, (fengman.jia@ucalgary.ca; ddlichti@ucalgary.ca; gyoungmin.kang@ucalgary.ca)
[2] Department of Chemical and Petroleum Engineering, University of Calgary, 2500 University Dr NW, Calgary, AB, T2N 1N4, Canada, (roman.shor@ucalgary.ca; arsh.khawaja@ucalgary.ca)
[3] Department of Mechanical Engineering, University of Calgary, 2500 University Dr NW, Calgary, AB, T2N 1N4, Canada, (maxwell.kepler@ucalgary.ca)

Key words: *sensor; LiDAR; laser scanning; drill bit grading*

ABSTRACT

Reservoir development in the petroleum industry starts with the drill bit. A drill bit's dull condition must be closely monitored since it significantly influences the efficiency and the cost of drilling operations. The dull condition check procedure is called drill bit grading and is essentially a change detection problem to determine the state of the drill bit, in particular the wear of the cutting teeth inserts. Currently, the grading is conducted manually on-site, which is error-prone and highly subjective. Laser scanning technology offers a potential solution to overcome the shortcomings of existing practice. The integration of LiDAR (Light Detection and Ranging) on the newly-launched iDevices, the iPhone 12 Pro and the iPad Pro 2020 offers new opportunities for close-range measurement given their huge customer base and low cost. The goal of this research is to investigate the performance of these devices, and to develop a tool for the drill bit grading. Since bit grading is significantly impacted by the performance of the sensor, several basic tests were first conducted under controlled experimental conditions, *e.g.*, the room temperature and ambient lighting and measurement surface. The temporal stability of the iDevices was examined by capturing a series of datasets of a flat wall over forty-five (45) minutes, then the effect of range, reflectivity and incidence angle on data quality was tested by measuring the Spectralon targets at different situations. The performance tests found that using only the LiDAR data was not sufficient for drill bit grading. Thus, a preliminary grading system based on the fusion of LiDAR and color camera is proposed by modelling the post-drilling bit and detecting the changes.

I. Introduction

Being used in the first step in reservoir development, drill bits play a critical role in petroleum industry. The drill bit is connected to the head of a rotary drill pipe and then transmitted downward to the well. According to the cutting mechanism, drill bits are broadly classified into two main types, rolling cutter bits and fixed cutter bits. The focus of this paper is a particular type of the fixed cutter bits, the Polycrystalline Diamond Compact (PDC) bit. This type of bit is usually made with a matrix or steel body. On the bit body, several blades are constructed with multiple cylindrical cutter inserts. The bit also contains nozzles that transmit drilling fluid during the work and includes other supporting structures.

Apart from the maximum drilling performance, another design goal that a drill bit must satisfy is a long service life. Thus, the dullness of a post-drilling bit needs to be assessed to identify the damage, to guide future bit selection, and thus to optimize the efficiency and cost of the drilling work. The industry standard for drill bit grading is published by the IADC (International Association of Drilling Contractors; Brandon *et al*., 1992). According to the IADC grading document, the dullness of a drill bit needs to be investigated in terms of several aspects including the primary cutting structure wear, overall gauge undersize, etc. A score or code is used to either measure or describe the damage condition in each aspect. A detailed introduction to the drill bit grading will be covered in Section III.

Up until now, most dull grading is conducted by a manual and highly subjective screening approach, which is error prone and inconsistent. Some research has been conducted to replace of this subjective procedure. Ashok *et al*. (2020) developed an image-based drill bit grading method by using the trained Convolutional Neural Networks (CNN) to identify the drill bit and image processing techniques in damage assessment. Ekeregbe *et al*. (2021) also proposed an approach using the deep learning, but the data analytics were based on a video that captures the drill bit in 360°.

As a technique that can remotely gather large volumes of 3D point information of an object, LiDAR has been used in widespread applications including surveying, autonomous vehicles, robotics, videogames, among others. The last two decades have witnessed a skyrocketing development of LiDAR, and laser scanning sensors have also experienced tremendous improvements in price, size, portability, and compatibility. The variety of the sensors ranges from terrestrial laser scanners to the mobile LiDAR backpacks, from the handheld systems to smart devices.

In 2020, Apple launched their first two devices with an embedded LiDAR scanner, the iPhone Pro 12 and the iPad Pro 2020 (hereafter denoted as the iPhone and the iPad). However, not much information has been unveiled on this custom-designed LiDAR sensor except that it improves the camera's properties and allows taking 3D measurements and point clouds of an environment up to 5 m away, at ns speeds (Apple, 2021). Limited research has been found on investigating the performance of Apple's LiDAR sensor. Among them, Luetzenburg *et al*. (2021) tested the technical capabilities of the iPhone and iPad by repeatedly taking scans for fourteen (14) rectangular boxes varied from 14 cm × 6 cm × 2 cm up to 50 cm × 30 cm × 52 cm. Comparing with the photogrammetric point cloud, both the accuracy and the precision of the iPhone's LiDAR were found to increase with the object size in all dimensions. They also reported an 11 cm cloud-to-cloud distance between the iPhone and photogrammetric solutions in modelling a coastal cliff of 130 m × 15 m × 10 m. Vogt *et al*. (2021) conducted an accuracy test of the LiDAR and TrueDepth cameras on iPad by imaging Lego bricks from 300 mm with a 65° scanning angle. However, it was found that the iPad's LiDAR camera was impractical for the capture of small objects due to the selection of the data collection application. A comparison between the iPad's LiDAR and a professional mobile laser scanner on measuring tree parameters was made by Gollob *et al*. (2021). The precision for the tree diameter estimation from iPad was found to be up to 4.5 cm, while it was 1.6 cm for the professional scanner. Research regarding the iPad's performance on the tree diameter measurement can also be found in Wang *et al*. (2021), which indicated a bias of up to 4 cm in scanning one hundred one (101) trees with diameters of 39.72 cm ±19.42 cm. Spreafico *et al*. (2021) compared iPad with the Faro Focus^{3D} X330 in the rapid architectural mapping. Their research implied that the iPad seemed promising as a portable cost-efficient solution, while 60% of the points achieved a less than 2 cm cloud-to-cloud distance.

The aim of our work is to first evaluate the iPhone and iPad's LiDAR sensors through a comparison with the industrial HDS6100 scanner manufactured by Leica, and then to determine the potential of these devices for drill bit modelling and dull grading.

This paper is structured as follows: the background of drill bit grading problems and the literature review for the LiDAR on Apple devices are provided in this section. In Section II, the performance of LiDAR on iPhone and iPad are investigated under controlled experiment environment. This includes the sensors' temporal stability during repeated tests over time and the range precision from various distances and incidence angles for objects having different reflectivity. A drill bit scanning strategy guided by the performance test outcome is described in Section III, followed by the post-processing of the captured model that includes the drill bit isolation and point cloud denoising. In Section IV, a preliminary drill bit grading method involving both LiDAR and 2D camera is proposed. Finally, conclusions are drawn, and some future topics are suggested in Section V.

II. LiDAR PERFORMANCE ANALYSIS

Several tests were conducted to examine the performance of the LiDAR integrated in the 2020 iDevices. The purpose of these tests is to quantify the quality of the lidar data and to further guide the data collection, so that the drill bit can be modelled precisely.

To mitigate the errors caused by environmental or personal factors, the following data capture method was used for all the tests in this section:

1. The devices were mounted on a tripod (Figure 1a and Figure 1b), and a plastic clamp mount was used to connect both devices to the tripod.
2. All the devices were operated by one person, under a controlled room temperature of 20.1℃ and a stable artificial lighting conditions.

Among the available data collection applications, SiteScape (SiteScape, 2021) was used because unlike other applications, it does not perform any extra processing such as meshing or interpolation on the raw data. For each test, another set of data was also collected with a high-accuracy, commercially-available scanner, the Leica HDS6100. With a modelled surface precision of 1 mm at 25 m, data from HDS6100 were used as a benchmark to assess the quality of data from the iDevices.

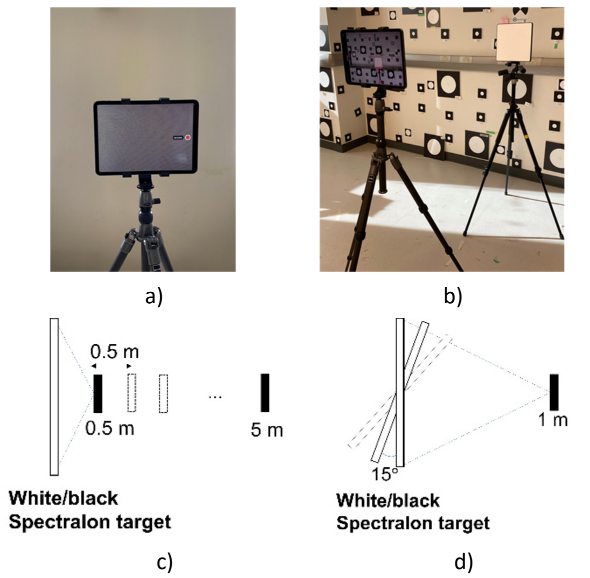

Figure 1. Experimental setup: a) Temporal stability tests; b) Range tests; c) Schematic diagram for the range, reflectivity, and incidence angle tests.

A. *Temporal stability analysis*

1) Experimental Description: All three devices (the iPhone, the iPad, and the HDS6100) were set up to image a flat wall at 1.5 m range (Figure 1a). The wall is constructed of drywall and painted matte beige. Scans of the wall were captured every one (1) minute for iPhone/iPad, and every five (5) minutes for HDS6100 for a period of 45 minutes.

2) Experimental results: Each dataset was checked by performing a least-squares plane fit. The results are presented in Figure 2. The RMSE (root mean square error) is a measure of the quality of the plane fit and can indicate the level of random noise in the system. The HDS6100 RMSE, which is consistently below 1.0 mm (Figure 2a), sets the benchmark for data quality and confirms the degree of flatness of the wall. The results for the iDevices have larger RMSE values, which indicate a higher degree of noise. However, with this setup, the iDevices can also provide millimetre-level precision, which is only slightly worse than the HDS6100. No obvious evidence indicates the necessity of a warm-up period to ensure the stabilization of the LiDAR data.

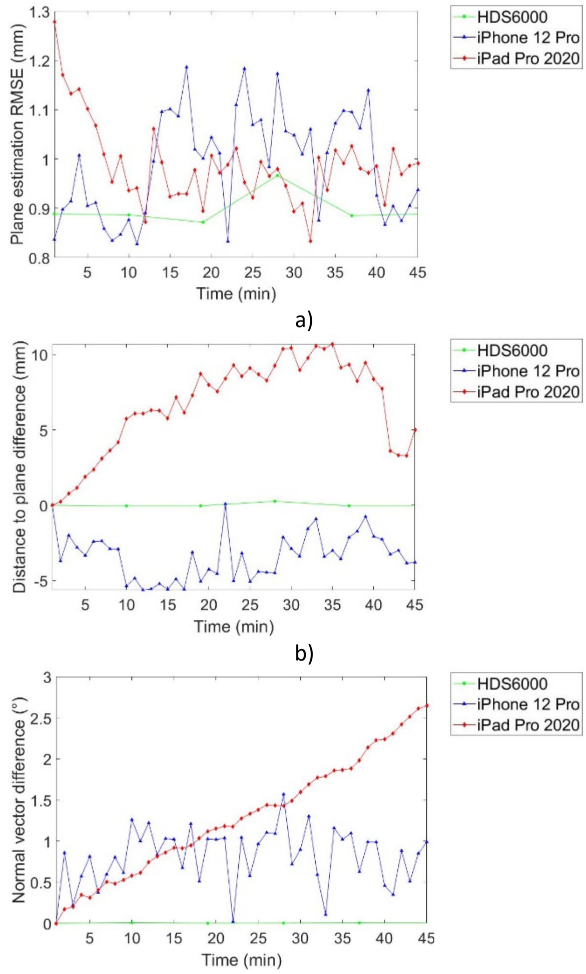

Figure 2. Temporal stability analysis: a) Plane fit precision; b) Distance to plane differences; c) Normal vector differences.

The device-to-plane orthogonal distance, and the normal vector of the plane were also estimated. When compared to the Leica HDS6100 reference, they can give an indication about the accuracy of reconstructing a planar surface in 3D. The results can identify instrument instability. The values reported in Figures 2b and 2c are the changes in orthogonal distance and normal vector orientation relative to the first data collection epoch. Values that are close to zero indicate a more stable reconstruction. The HDS6100 reference parameter values are clearly very stable, with little discernable change over time. One can see that the iDevices' results are less stable, especially the iPad. Figure 2c shows a clear trend of growing normal vector instability in the iPad. This could be from the wobble of the clamp that was caused by touching the screen for data collection. Physically touching the screen is necessary to commence the LiDAR data collection. That said, it is also possible that sensor instability contributes to the visible trend. Further investigation is required to test this hypothesis.

B. *Range, reflectivity, and incidence angle analysis*

1) Experimental Description: Two 27 cm × 27 cm Spectralon targets were used to test the impact of range, reflectivity, and incidence angle on the LiDAR performance. The white target (Figure 1b) has 99% reflectivity and the black target has 25% reflectivity. Spectralon targets are used due to their nearly constant spectral reflectivity in the visible and NIR (near infrared) part of the spectrum and their near-Lambertian behaviour. Each the targets were imaged at normal incidence every 0.5 m from 0 m to 5 m as shown in Figure 1c. Then, the tests were repeated at 1 m but with various incidence angles to the target surface: every 15° from 0° to approximately 82° as shown in Figure 1d. Point clouds captured with each sensor were manually cropped so that only points lying within the extents of the Spectralon target were used in the plane fitting. Although the Spectralon target materials are quite different from that of drill bits, as accepted reference standards they give an indication of best-case data quality that can be expected.

2) Experimental results: Like the temporal stability tests, the plane fit precision was estimated to evaluate the LiDAR's range precision under different scenarios. As can be seen from Figure 3a, the target can only be measured up to a 4 m range with the iDevices. The working range for the iPhone/iPad's LiDAR is reported as up to 5 m. The Leica HDS6100 reference provides better than millimetre precision at distances above 1.5 m, which is consistent with its reported modelled surface precision of 1 mm at up to 25 m.

Poorer precision can be found at the closer distances for HDS6100, which is caused by placing the object within the reported minimum working range of the scanner, which is 1 m in this case. The range precision for iPhone and iPad decreases with distance, and a 5 mm precision can be achieved if the object is captured within a 1.5 m range. Interestingly, the results for the black and the white targets are very similar. However, the RMSE values for the white Spectralon are larger than those from the wall test. This may be due to the higher reflectivity of the reflectance standard. The plots of plane fit residuals in Figure 3b indicate the “flatness” of the captured target. Green dots represent points that lie on the plane, while red and blue points represent points that deviate significantly from the estimated plane. These results show that the range measurements above 1.5 m do not accurately represent the shape of the flat Spectralon target.

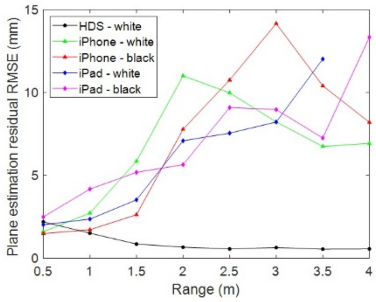

a)

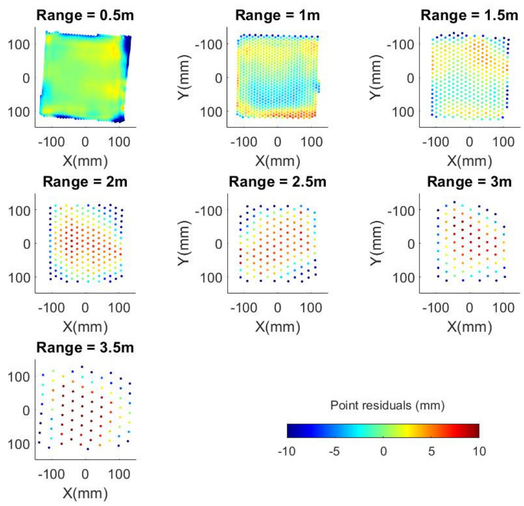

b)

Figure 3. Impact of range on data quality: a) Plane fit precision; b) Plane fit residuals.

Plane fit precision from the incidence angle tests is shown in Figure 4. The reference data results from the HDS6100 are again of very high quality. The number and geometry of iDevice data points decreases dramatically at high incidence angles (above 45°). However, deeper investigation is required to uncover the cause of the spikes at 45°. Thus, the planes cannot be reliably estimated from the captured data. Results above this incidence angle should not be considered. Analysis of the remaining data reveals that the data captured at incidence angles below 30° exhibit compatible precision. Regarding the reflectivity, no significant differences has been observed in the data captured from the two targets.

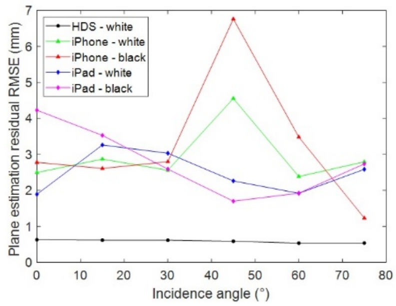

Figure 4. Plane fit precision from the incidence angle tests.

III. The modelling of drill bit

A. *Introduction to the drill bit*

As mentioned before, the fixed cutter PDC bit is the object of this research. Different PDC bits may vary in size and shape, but they have the similar primary cutting structure, which consists of several blades with PDC cutters inserted on each of them. On the PDC bit shown in Figure 5a, six (6) blades can be found, while four (4) to six (6) cutters are fixed on each blade. The dimensions of the bit and cutters are approximately 20 cm (L) × 20 cm (W) × 15 cm (H) and 1 cm (L) × 1 cm (W) × 1 cm (H), respectively.

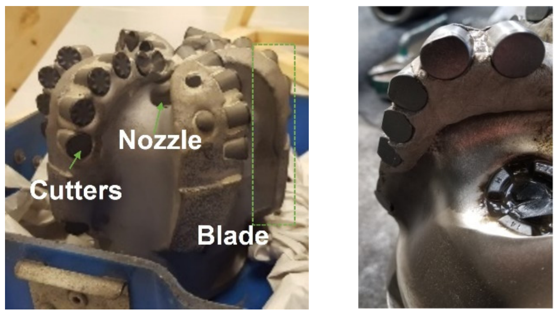

a) b)

Figure 5. A PDC drill bit: a) Unused drill bit; b) Used drill bit with cutter wear.

According to the IADC regulation, the grading of a fixed cutter drill bit needs to be conducted in terms of the following four aspects:

1. Cutter wear. Figure 5b shows a PDC bit after removal from the drilling hole. Different levels of cutter wear can be observed. According to IADC, the cutter wear should be graded following the scale illustrated in Figure 6. By considering the cutter surface as a circle, it scores the cutter wear by estimating the worn amount of the circle. According to the grading scale between 0-8 listed in Table 1, the more the wear is, the higher the grade would be.
2. Primary dull characteristic and location. This is the description of the primary damage on the bit, *e.g.*, lost cutters or worn cutters. The corresponding location is also recorded.
3. Gauge undersize. This test is conducted by placing a gauge ring over the largest diameter of

a post-drill bit and measuring the gap in between.

4. Remarks. This includes the second most notable condition and the possible reasons for all the damages.

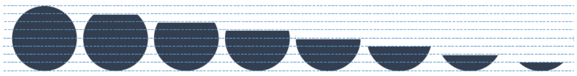

Figure 6. Schematic diagram for the cutter wear grading scale (BESTEBIT, 2021).

Table 1. Cutter wear grading scale

Grade	0	1	2	3	4	5	6	7	8
Wear	$\frac{0}{8}$	$\frac{1}{8}$	$\frac{2}{8}$	$\frac{3}{8}$	$\frac{4}{8}$	$\frac{5}{8}$	$\frac{6}{8}$	$\frac{7}{8}$	$\frac{8}{8}$

Following this IADC standards, this paper focuses on the grading of the primary cutting structure, which is the wear of the cutters. The overall goal is to replace the current subjective grading procedure with a more accurate and consistent method using an imaging sensor such as one of the iDevices.

B. *Suggested drill bit modelling procedure*

According to the performance tests, the LiDAR from the iPhone/iPad has been found to perform best when the object is scanned within 1.5 m and with an incidence angle that is smaller than 30°. The SiteScape app integrates the IMU (Inertial Measurement Unit) data for real time registration while moving the device, thus provides a registered 3D model of the object.

Based on the above conditions and several test scans, the authors found that instead of scanning the entire drill bit (Figure 7a), which leads to many mixed-pixel errors, higher data quality can be achieved if the drill bit is scanned blade by blade (Figure 7b). As the cutters are distributed on the top half of the drill bit (Figure 5), it is recommended to start scanning from the top of each blade and gently move the devices to the bottom. By doing so, the registraion errors can be mitigated for the the best results.

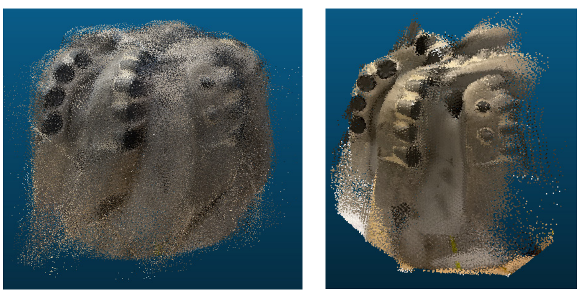

a) b)

Figure 7. Drill bit and the test scans: a) Full drill bit scan; b) Single blade scan.

C. *Drill bit model post processing*

The scanned model needs to be processed before being analyzed. This post-processing mainly includes the following two steps.

1) Drill bit model segmentation: Figure 8a shows a raw point cloud from a larger standoff distance and includes unwanted measurements in the background. Thus, the drill bit needs to be identified in the point cloud. Assuming that the drill bit was within a 1.5 m range of the devices, the drill bit isolation was realized by firstly removing points at longer ranges. Then, the remaining point cloud was segmented based on the colour information to separate the drill bit from other objects. Lastly, the segmented point cloud was extracted by connected components analysis. The largest cluster was saved as the identified drill bit model (Figure 8b). Note that the bit shown in Figure 8 has no PDC cutter bits. All bits were removed and replaced by with artificial bits made from wooden dowels to allow simulation different wear conditions.

2) Point cloud denoising: The point cloud denoising is required due the existence of outliers, many of which are mixed pixels. This was realized by the statistical outlier removal method. The idea of this method is that it will first calculate the average distance from each point to its fifty (50) nearest neighbours, which are found by the k-d tree method. Then, a distance threshold will be defined as the mean plus deviation of all these average distances. Points whose average neighbour distance are above this threshold will be considered as outliers and will be removed from the point cloud. The denoised drill bit model is shown in Figure 8c.

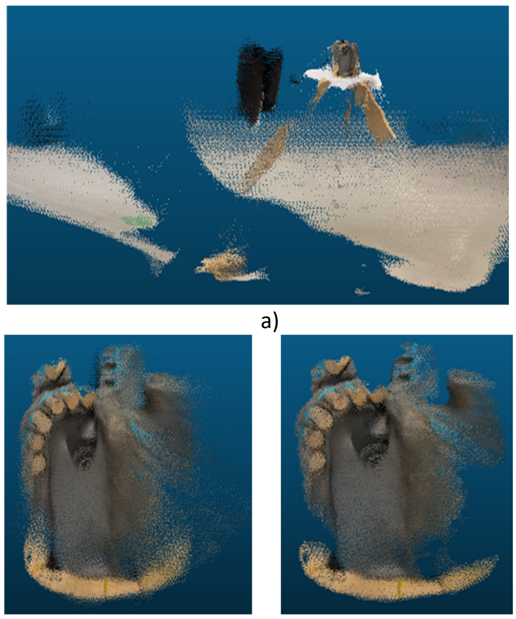

a)

b) c)

Figure 8. Point cloud post processing: a) A sample scan from iPhone; b) Isolated drill bit scan; c) Denoised drill bit model.

IV. Drill bit grading strategy

The initial plan of this research was to test the performance of the LiDAR sensor on the new iDevices, and to determine the potential of using only one sensor to fulfill the goal of drill bit grading. However, based on our experimental findings, the LiDAR on theses smart devices only captured the general geometry of the drill bit and was not capable allowing identification of the finer details like the wear of the cutters. This was largely due to mixed pixel data artefacts and registration errors from the IMU data. Thus, a drill bit grading technique presented in this paper also utilizes the iPhone/iPad colour camera images. The LiDAR data are used to provide 3D information that can improve the 2D-only solutions. One picture needs to be taken for each blade from a proper perspective, after which the following steps are performed to grade the cutter wears.

A. *Image ortho-rectification*

Ortho-rectification is the process of synthetically generating an orthophoto, which is an image of the object space in orthogonal parallel projection. By doing so, the distortions due to image tilt and relief displacement can be corrected.

Image ortho-rectification is essentially the process of transforming a central-perspective digital image by the analytical funtions f_x and f_y in Equation 1, and assigning the color in the corresponding pixels (Novak, 1992). This can be done by either direct or indirect method as described by Equation 1.

$$x = f_x(x', y')\ ;\ y = f_y(x', y') \tag{1}$$

where direct transformation means if:

$x, y =$ pixels of the orthophoto
$x', y' =$ pixels of the original image

and indirect transformation means if:

$x, y =$ pixels of the original image
$x', y' =$ pixels of the orthophoto

Since the direct method transforms the pixels on the original image to the orthophoto, it may happen that some pixels on the orthophoto have no correspondences on the original image and no color value can be assigned. Thus, the indirect method is more commonly used.

Among all the ways to determine the analytical function, a method is called projective transformation. This method is used if the object scene can be modelled as a plane, then the problem is reduced to mapping the pixels of the orthophoto plane into the original image (Figure 9).

The projective transformation models the geometric relationship between two planes. It is defined by eight (8) parameters from a_1 to c_2 in Equation 2. It can be solved by using four (4) control points lying in a plane in the object space and their corresponding pixels in the original image.

$$\begin{aligned} x &= \frac{a_1 x' + a_2 y' + a_3}{c_1 x' + c_2 y' + 1} = f_x(x', y') \\ y &= \frac{b_1 x' + b_2 y' + b_3}{c_1 x' + c_2 y' + 1} = f_y(x', y') \end{aligned} \tag{2}$$

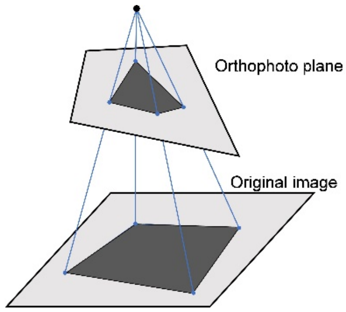

Figure 9. The projective transformation between the orthophoto plane and the original image. Four (4) points are required to solve the transformation function.

An image for the drill bit in Figure 10a was taken at a perspective that best captured the cutters on an individual blade. One can see that the circular shaped cutter surfaces were elongated to ellipses to different extents. As the cutter surfaces lie roughly on a plane in object space, the ortho-rectification can be done by using the projective transformation method. The 3D coordinates of the cutter centers were extracted from the previously generated LiDAR model, and then were transformed into the 2D pixel coordinates in the orthophoto. When combined with the coordinates in the distorted image, the transformation fucntion parameters were estimated. By applying the transformation parameters to every pixel, the ortho-rectified image was generated. As shown in Figure 10b, the cutters have been mostly corrected to their true shapes, which are circles in this case. Some residual deformation to the circles still exists due to the deviation of the cutter surfaces from the hypothesized planar shape.

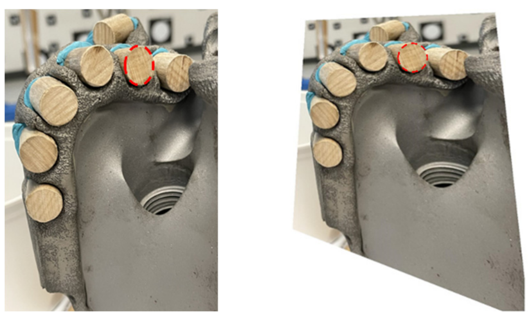

a) b)

Figure 10. Image ortho-rectification: a) The original image; b) Rectified orthophoto.

B. *Circle detection and isolation*

The cutters were replaced by the worn ones for the following grading procedure. They were identified in the rectified image by considering them as individual circles. Each circle was detected by the circular Hough transform. Six (6) cutters were detected on the blade in Figure 11a. Even though cutter 5 is partially occluded, its circumference can still be partially extracted and the wear measurement made. With the estimated centers and radii, each cutter can be cropped out from the Image for the following grading procedures. The isolated cutter images are shown in Figure 11b.

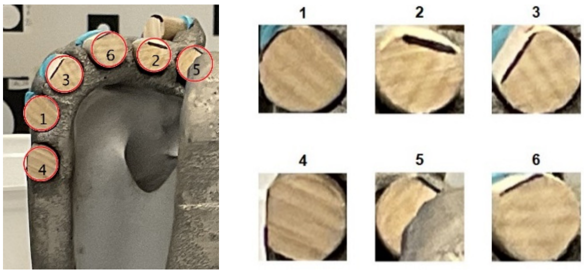

a) b)

Figure 11. Circle detection. a) Detected circles; b) Isolated cutter images.

C. *Cutter wear grading*

The key point of the cutter wear grading is to recognize the edge that represents the location of wear. When using the artificial wooden cutter bits, accurate detection of the edge requires the aid of the edge marks as shown in Figure 11b. The edges were marked with black indelible marker to highlight the wear edges on the cutters so that they can be more easier detected in the image. The process for cutter wear grading can be summarized as the following three steps.

1) Detection of the edge: Pixels with a certain colour, *i.e.*, black in this case, were detected as the potential edge points. Shadows were excluded by removing the points that are overlain with the detected circles. Next, the largest connected component was labelled as the edge of the cutter wear, as can be seen in Figure 12.

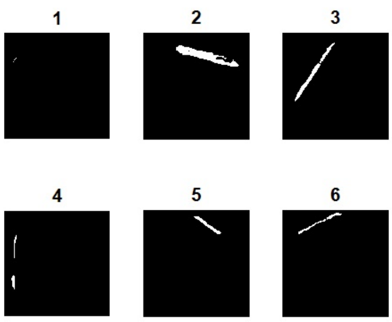

Figure 12. The detected edge of the cutter wear.

2) Edge "recovery": By using the points found in the last step, lines that represented each edge were estimated. Two intersection points between the line and the circle, marked as the blue and red triangles in Figure 13, were found for each edge to indicate the location of the cutter wear.

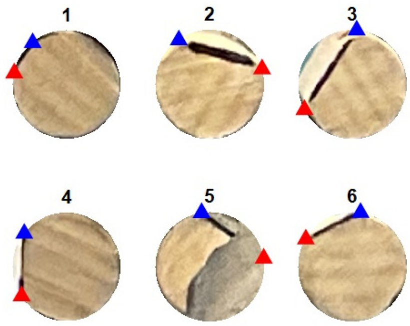

Figure 13. Edge "recovery" results.

3) Wear estimation: Following the grading strategy in Figure 6, the amount missing from each circle, which indicates the amount of cutter wear, is estimated. Table 2 lists the estimated wear of each cutter in Figure 13, and their grades determined based on Table 1. The value between two grades was rounded to the closer one.

Table 2. The estimated wear and grades.

ID	1	2	3	4	5	6
Wear	$\frac{0}{8}$	$\frac{2}{8}$	$\frac{2}{8}$	$\frac{1}{8}$	$\frac{1}{8}$	$\frac{1}{8}$
Grade	0	2	2	1	1	1

V. CONCLUSION

The current widely-used approch for grading a drilling bit is by visual inspection, which can be highly-subjective and inaccurate. Thus, a consistent and ideally automated solution is expected. The aim of this work was to develop a new remote sensing approach using the new Apple iDevice LiDAR sensors, which have made 3D point clouds accessable with consumer-level devices.

In this paper, several performance tests were first conducted on the new sensor. Results from the temporal stability test reveal that the iDevices provide millimetre-level precision in plane modelling at a range of 1 m, which is only slighly worse than the reference data results from the Leica HDS6100 scanner. It has also been found that the performance of the iDevice LiDAR is more greatly impacted by the range than by the incidence angle and the object's reflectivity, which suggests an ideal scanning configuration of within a 1.5 m range and a 30° scanning angle.

According to the performance tests, it was found that more research needed to be done to realize the drill bit grading by only using the LiDAR. Thus, colour camera imagery was introduced in the proposed method. 3D information from LiDAR was used to help reduce the image distortion and to improve the results from image processing. Experiment results on laboratory data show that drill bit grading is possible using the proposed new image based method.

Future work will be to pusue the LiDAR-only solution. As Apple doesn't publish the sensor's specifications, more comprehensive research needs to be implemented. It may include an application development so we can have direct access to the sensor and data. After that, more tests could be done regarding, for example, the scanning resolution, the measurement accuracy, the impact of placement angle of the device, the LiDAR sensor calibration. If the LiDAR data is sufficent for drill bit grading, new methodologies need to be proposed including the data registration, cutter segmentation and modelling. If not, the generated bit model can still be used to improve the current ortho-rectifciation results. Last but not the least, machine learning can be applied on the improved orthophoto to achieve more accurate image-based solution.

VI. Acknowledgements

This project was funded by the Natural Sciences and Engineering Research Council (NSERC) of Canada (ALLRP 561422 – 20 and RGPIN-2018-03775).

References

Apple Inc. (2021). Apple Unveils New iPad Pro with Breakthrough LiDAR Scanner and Brings Trackpad Support to iPadOS. https://www.apple.com/ca/newsroom/2020/03/apple-unveils-new-ipad-pro-with-lidar-scanner-and-trackpad-support-in-ipados/. Retrieve date 22-Nov-2021.

Ashok, P., P. Vashisht, H. Kong, Y. Witt-Doerring, J. Chu, Z. Yan, E. van Oort, and M. Behounek (2020). Drill Bit Damage Assessment Using Image Analysis and Deep Learning as an Alternative to Traditional IADC Dull Grading. In: *SPE Annual Technical Conference and Exhibition*. OnePetro.

BESTEBIT (2021). IADC Dull Grading for PDC Drill Bits. https://www.bestebit.com/wp-content/uploads/2016/12/PDC-Dull-Grading.pdf. Retrieve date 22-Nov-2021.

Brandon, B.D., J. Cerkovnik, E. Koskie, B. B. Bayoud, F. Colston, R. I. Clayton, M. E. Anderson, K. T. Hollister, J. Senger, and R. Niemi (1992). First Revision to the IADC Fixed Cutter Dull Grading System. In: *IADC/SPE Drilling Conference*.

Ekeregbe, M. P., M. S. Khalaf, and R. Samuel (2021). Dull Bit Grading Using Video Intelligence. In: *SPE Annual Technical Conference and Exhibition*. *OnePetro*.

Gollob, C., T. Ritter, R. Kraßnitzer, A. Tockner, and A. Nothdurft (2021). Measurement of Forest Inventory Parameters with Apple iPad Pro and Integrated LiDAR Technology. *Remote Sensing*, Vol. 13, No.16, pp. 3129.

Luetzenburg, G., A. Kroon, and AA. Bjørk (2021). Evaluation of the Apple iPhone 12 Pro LiDAR for an Application in Geosciences. *Scientific reports*, Vol. 11, No. 1, pp. 1-9.

Novak, K. (1992). Rectification of Digital Imagery. *Photogrammetric Engineering and Remote Sensing*, Vol. 58, pp. 339-339.

SiteScape (2021). SiteScape Hompage. https://sitescape-test.webflow.io/. Retrieve date 15-Nov-2021.

Spreafico, A., F. Chiabrando, L. T. Losè, and F. G. Tonolo (2021). The Ipad Pro Built-In LIDAR Sensor: 3d Rapid Mapping Tests and Quality Assessment. In: *The International Archives of Photogrammetry, Remote Sensing and Spatial Information Sciences*, Vol. 43, pp. 63-69.

Vogt, M., A. Rips, and C. Emmelmann (2021). Comparison of iPad Pro®'s LiDAR and TrueDepth Capabilities with an Industrial 3D Scanning Solution. *Technologies*, Vol. 9, No. 2, pp. 25.

Wang, X., A. Singh, Y. Pervysheva, K. E. Lamatungga, V. Murtinová, M. Mukarram, Q. Zhu, K. Song, P. Surový, and M. Mokroš. (2021). Evaluation of Ipad Pro 2020 LIDAR for Estimating Tree Diameters in Urban Forest. In: *ISPRS Annals of the Photogrammetry, Remote Sensing and Spatial Information Sciences*, Vol. 8, pp. 105-110.